Particle engineering of gypsum through templating with starch

Sebastian J. Gurgul [a], Gabriel Seng [b] and Gareth R. Williams [a]*

[a] UCL School of Pharmacy, University College London, 29-39 Brunswick Square, London, WC1N 1AX, UK

[b] Etex Group, 500 Rue Marcel Demonque, Avignon, 84000, France

* Corresponding author. Email: gwilliams@ucl.ac.uk

KEYWORDS: templating, gypsum, starch, setting time, liquid seeds

ABSTRACT

The conversion of $CaSO_4 \cdot 0.5H_2O$ to $CaSO_4 \cdot 2H_2O$ (gypsum) is of great importance industrially, being the reaction behind plasterboard production and the setting of medical plasters. This hydration process is inherently slow, and to ensure that it occurs on a practical timescale "seeds" of gypsum are typically added to accelerate the reaction. The seeds used in industry are mostly produced by milling quarried gypsum, resulting in huge variations in their accelerant properties between batches. Here we develop a bottom-up process to prepare gypsum seeds with tightly defined morphology, using starch as a templating agent during precipitation from water/ethanol mixtures. When the seeds thereby generated are dried, they tend to aggregate, which results in diminished accelerant properties. The hydration (or setting) time can be markedly reduced if these aggregates are broken up and suspended in a liquid

medium. This indicates that directly adding the suspension reaction product to an industrial production line could be a powerful way to accelerate the setting reaction. However, the use of ethanol in the seed synthesis precludes this (since the ethanol would halt the setting reaction). Therefore, a direct one-step process involving evaporation of ethanol was developed to produce gypsum seeds in a water suspension with no ethanol present. The resultant "liquid seeds" are highly potent in accelerating the hydration process of $CaSO_4 \cdot 0.5H_2O$ to $CaSO_4 \cdot 2H_2O$, resulting in shorter setting times than a commercial standard gypsum accelerant.

1. Introduction

Plasterboard or drywall comprises a gypsum (calcium sulfate dihydrate, CSD) core sandwiched between two layers of lining paper. The inclusion of various additives (e.g. glass fibre, plasticizers, foaming agents, or chemicals to increase fire resistance) in the CSD layer, and varying the weight and strength of the outer paper, will give the finished board different properties.[1–3] Plasterboard is used extensively as an indoor building material because of its simple and cheap fabrication process, fire resistance, environmental friendliness and low price.[4] Commercially, plasterboard is prepared by taking calcium sulfate hemihydrate (HH) and mixing with water to generate a slurry. The slurry is injected between two sheets of paper and left to react on a long conveyor belt, ultimately producing solid CSD ("setting"). During the latter stage of the process, around one third of the surface water is evaporated, and the plaster hardens.

Any residual water left at the end of the line must be removed by a heat treatment, which is both expensive and time consuming. However, this step is crucial because incomplete hydration causes a loss of mechanical strength in the final product.[5] To speed up the conversion from hemihydrate to dihydrate, seed crystals of CSD are generally added to the HH slurry; these are thought to provide extra nucleation sites, and have the additional benefit of improving

the hardness of the plaster.[6] To prepare such seeds, factories use a simple grinding process. However, a range of different types of mills (e.g. ball mill, vertical roller mill, hammer crusher) can be used, produced by a wide range of suppliers. Further, the use of different processes and gypsum sources means that the seeds generated are different at each location, and thus have varied behaviour in terms of accelerating the hydration process.[7–10] At a constant mixing ratio of plaster and water, differences of 10 to 20 % can be observed in the mechanical properties of plasterboards generated using accelerators produced by grinding. There are also smaller changes in the density of the products obtained (in the range of 1 %). By way of example, the setting times of a number of batches of molding plaster produced by Etex Group in France are shown in the Supporting Information (Figure S1). The setting time falls in the range of 8 to 15 minutes, with corresponding variations in the final mechanical strength of the solid structure obtained (with variations of about 15 % around the mean value).

It also leads to issues with setting up a new factory or when working with a new gypsum source, as every time significant optimisation will be required to determine the appropriate milling parameters and the correct amount of seeds to use for setting. There is thus a great need to standardise the production of gypsum seeds, to ensure batch-to-batch quality control. The method must be reproducible, cost-effective, and efficient. A “bottom-up” route to seed generation could have major benefits in terms of producing more homogeneous seeds, and allowing all factories to prepare materials with known properties using the same recipe.

Solvent-based templating is one approach which has been successfully employed in the precipitation synthesis of CSD. For instance, use of different concentrations of citric acid changes the particle habit from needles into aggregates composed of leaf-like crystals.[11,12] The addition of organic solvents such as ethyl acetate, glycerol, isopropyl alcohol, dimethylformamide or propylamine also has a significant effect on the morphology of the particles generated, giving habits ranging from rod-shaped to flat and flower-shaped particles.[13]

When D,L-maleic acid is present in the solution the CSD product tends to take spearhead-like shapes.[14] The addition of polymers also has an effect on gypsum particle habit. Lioliou et al. explored this effect with polyacrylic acid (PAA) of different molecular weights (2k, 50k and 240k).[15] In the presence of PAA, the crystals tend to agglomerate and have more plate-like shapes than the needles formed without a template. The literature thus shows that the use of habit modifiers can allow gypsum crystals with a specific shape and size to be prepared. However, to date there are no studies exploring the HH → CSD acceleration effects of the templated materials or investigating the correlation between particle habit and setting time properties.

In this work, we sought to develop a simple and environmentally-friendly templating route to generate potent gypsum seeds, with a focus on ensuring translatability to the factory floor. As a templating agent, we selected a soluble starch; this has successfully been used to template size- and shape-controlled silver and gold nanoparticles,[16] is available commercially in large quantities from renewable resources,[17–19] and can easily be removed from the CSD product by washing in water.

2. Materials and methods

2.1. Materials

Calcium chloride was purchased from Sigma-Aldrich, sodium sulfate from Fisher Scientific, and modified starch (insoluble content below 0.01%, lot P01F012) from Alfa Aesar. Ethanol was sourced from VWR International. Ball-milled accelerant, BMA, is composed of raw gypsum mixed with additives such as starch, sugars, glycerin, and a range of salts.[7–10] The BMA used in this work was supplied by Etex Ltd and prepared at their Mériel site in France by milling raw gypsum with starch. α- and β-hemihydrates were standard non formulated molding plasters produced by the Mériel factory.

2.2.Synthesis

2.2.1. Dry seeds

In all syntheses, the solvent was a mixture of ethanol and water (30/70 v/v). Separate 0.1 M solutions of calcium chloride and sodium sulfate were prepared, and with or without starch as a templating agent. The mixtures were stirred at room temperature (RT) for 30 min to ensure complete dissolution. 100 ml of the sodium sulfate solution was then rapidly added to 100 ml of the solution of calcium chloride (since dropwise addition could lead to different nucleation start times). The resultant mixture was stirred for 10 min before being allowed to stand for 24 h at room temperature, prior to recovery of the solid product through vacuum filtration. The solid precipitate was washed with 4 × 75 ml of deionised water and left to dry at room temperature for 24 h. All experiments were performed at least in triplicate.

2.2.2. Suspension formation

The dried seeds were suspended in a supersaturated solution of calcium sulfate hemihydrate (SSS). The latter was prepared by adding dry hemihydrate (100 g) to water (2 L), mixing at RT for 12 h, and then resting the suspension for another 12 h. The liquid was centrifuged at room temperature for 1 h at 9000 RPM, and the top layer (30 ml from a 50 ml tube) used as the SSS. Solid seeds were added to 2 ml of the SSS (giving a seed concentration of 5.6 % w/v with respect to the amount of water), sonicated for 15 min, and used as ‘liquid’ seeds (LS). A sample of the suspended seeds was recovered from the suspension by filtration for further analysis.

2.2.3. One-step preparation of seed suspensions

Two elevated temperatures were explored for the one-step synthesis. All experiments were prepared in ethanol/water (30/70 v/v). Separate 0.1 M solutions of $CaCl_2$ and Na_2SO_4 were made up. Modified starch (5% w/v was added to both). The solutions were stirred in sealed vessels at 75 or 80 ^oC for 30 min to ensure complete dissolution. 100 ml of the Na_2SO_4 solution was then rapidly added to 100 ml of the solution of $CaCl_2$ and the mixtures maintained at 75 or 80 ^oC. The reaction vessel was left unsealed at this point, to allow evaporation of ethanol. 3 ml samples were removed from the vessel periodically, centrifuged at 9500 RPM for 1 h at 6 ^oC, and 1 ml of the supernatant was transferred to a gas chromatography (GC) vial for analysis. The processes were performed in sextuplicate and the data reported as mean ± S.D. Once the time taken to remove the ethanol from the reaction mixture had been determined, the reaction was repeated without aliquots being taken, stopped when the residual ethanol content should have reached zero, and the resultant suspension used for onward experiments. A sample of the solid seeds was recovered by filtration for analysis. A second set of experiments was performed in which 100 ml of the Na_2SO_4 and 100 ml of the $CaCl_2$ solutions were combined at room temperature, before the temperature was elevated to 80 ^oC and stirring continued for 4 h.

2.3.Analysis

2.3.1. Materials characterization

X-ray diffraction (XRD) measurements were recorded on a Rigaku MiniFlex 600 diffractometer using Cu Kα radiation. Thermogravimetric analysis (TGA) was performed with a TA Instruments Discovery instrument. Samples were heated from 40 to 350 ^oC with a heat ramp of 10 ^oC/min, under a 25 ml/min nitrogen flow rate. Scanning electron microscopy was undertaken on a FEI Quanta FEG 200 instrument, after sputter-coating with gold. Fourier transformed IR (FTIR) spectra were recorded using a Perkin-Elmer Spectrum 100 instrument (resolution 4 cm^{-1}).

2.3.2. Gas chromatography

GC was undertaken using an Agilent GC 7890A instrument with an Agilent HP-5 column (5% phenyl methyl siloxane, model 19091J-413, diameter = 320 μm, film thickness = 0.25 μm; length = 30.0 m, void volume = 2.031 min; maximum temperature 325 °C). The settings for the GC were as follows: the oven was rapidly heated to 35 °C, then at 3 °C/min to 80 °C and 20 °C/min to 150 °C; split ratio 1:1; split flow: 1.5 mL/min; Carrier gas: nitrogen at 6 ml/min; injection volume: 0.5 μm. The total run time was 18.5 min.

2.3.3. Setting time quantification

These were performed with both the α- and β- forms of $CaSO_4 \cdot 0.5H_2O$. For α-plaster 70 g of α-HH was added to 28 g of water and mixed by hand for 1 minute, resulting in a plaster/water ratio of 250 %. For beta plaster 45 g of beta HH were added to 36 g of water and mixed by hand for 1 minute, resulting in a plaster/water ratio of 125 %. Seeds were added at a concentration of 0.2 % w/w with respect to the amount of hemihydrate (0.14 g and 0.09 g for α-HH or β-HH respectively) to the mix 30 s after the mixing started. The slurry was then poured into a disc mould (height 5 cm; radius 1.5 cm; volume 35.34 cm^3) and the mould lifted. A knife was used to cut through the disc every minute. Once the sides of the cut stopped coming together, the time was recorded as the setting time. Experiments were performed at least in triplicate, and results are reported as mean ± S.D. For liquid seeds, 70 g of α- or 45 g of β-calcium sulfate hemihydrate was added to 26.4 g (for α-HH) or 34 g (β-HH) of water, and mixed by hand. Liquid seeds were added to the mix after 30 s of mixing, and mixing continued for another 30 s. Again seeds were used at 0.2 % w/w with respect to the amount of hemihydrate (for α-HH 0.14 g of seeds in 1.6 ml of SSS, for β-HH 0.09 g of seeds in 2 ml of SSS). The slurry was then poured into a disc mould (height 5 cm; radius 1.5 cm; volume 35.34 cm^3) and

the mould lifted. The knife method was then used to determine the setting time, as detailed in the S Information, Figure S2.

2.3.1. Mechanical strength

Gypsum beams were prepared by mixing 780 g of α-HH with 312 g of water and 0.2 % w/w (with respect the amount of HH) of seeds, or 540 g of β-HH with 432 g of water and 0.2 % w/w seeds in moulds of 2 cm x 2 cm x 20 cm. The beams were airdried for at least 5 days in RT. Priory to analysis beams were dried at 45 ^{o}C for 24 hours. Full details are given in Table S 1 and Table S 2. For the bending test a gypsum beam was suspended between two stationary points 14 cm apart and pressure applied to the centre of the beam. For compression tests, a gypsum beam (2 cm height, 2 cm width and 4 cm long) was crushed between two plates. Both the flexure (bending) and compression tests were performed on an Ibertest ELIB /5 EW instrument. At least 5 measurements were taken and values are given as mean ± S.D.

3. Results

3.1. Templated seeds

Initial optimisation of the synthesis process explored a range of different concentrations of ethanol in water (10 – 40 % v/v). 30 % v/v ethanol was chosen for all subsequent syntheses because it maximised the yield from the process without compromising the solubility of the Na_2SO_4 (which did not dissolve fully in the 40% v/v water/ethanol system). Solutions were then prepared containing a range of starch concentrations and employed to generate gypsum seeds. The yields are shown in Table 1.

Table 1. Yields of samples generated using modified starch. TA = templating agent.

Template concentration	Yield (%)	Template concentration	Yield (%)
No TA	73 ± 3 %	10% w/v	92 ± 2 %
1% w/v	89 ± 2 %	15% w/v	90 ± 4 %
2.5% w/v	89 ± 1 %	20% w/v	56 ± 4 %
5% w/v	93 ± 4 %		

The yield is generally very high for all the starch-templated systems and exceeds 89% in all cases apart from the seeds synthesised with 20 % (w/v) starch. This is due to the fact at in this concentration the liquid is very viscous and extra water was needed to wash the seeds, resulting in some seeds being dissolved and lost. The yield was notably lower when no templating agent (TA) was employed.

XRD, FTIR and TGA data for the starch-templated seeds are given in Figure 1. The XRD patterns for the starch-templated samples clearly match the reference pattern[20] demonstrating the successful synthesis of CSD (Figure 1(a)). The reflections can be fully indexed using the gypsum unit cell[21] as summarised in Table S 3. It is worthy of note that the samples synthesised with starch have much stronger reflections at 20.76° 2θ (021) than at 11.66° (020), while the reverse is true for untemplated CSD (marked with arrows in Figure 1(a)). This suggests a different crystal habit, likely to be a result of the coils in the starch molecules acting as a habit modifier.

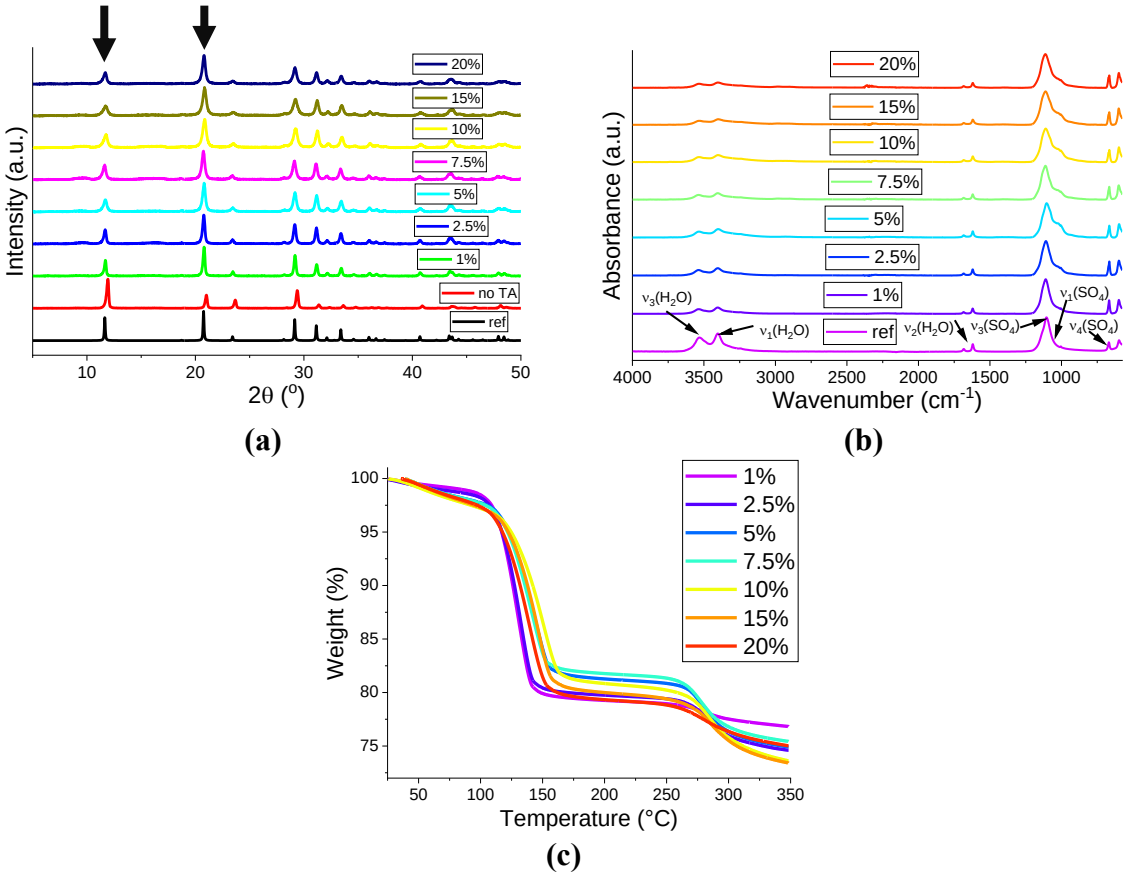

Figure 1. Characterising data for the seeds formed with different concentration (% w/v) starch solutions. (a) XRD; (b) FTIR; and (c) TGA data. Reference (ref) datasets are plotted based on data from (a) ref 20, and (b) ref 22.

The FTIR spectra (Figure 1(b)) clearly show the successful synthesis of gypsum, with vibrations arising from water and sulfate groups evident. A full assignment of the vibration bands is presented in Table S 4.[23] All expected bands are present in all the spectra, which agree with the reference spectrum.[22] At temperatures around 100 °C, gypsum loses ca. 21 % of its mass due to the loss of two water molecules per formula unit. The TGA data are presented in Figure 1(c), and the percentages of mass lost in the first step (measured at 250 °C) are summarised in Table S 5. In all cases, the mass lost in the first stage is very close to the calculated amount, again confirming the successful synthesis of gypsum. There is a small reduction in the mass loss when starch is used, potentially indicating the incorporation of the TA in the solid reaction product.

Following the confirmation that the solid material precipitated was gypsum, the starch-templated samples were then analysed using SEM. The images obtained are presented in Figure 2. Gypsum precipitated in the absence of starch has needle- and platelet-shaped particles which are loosely aggregated. With starch, the particles are again mostly needle shaped. At low concentrations (1 – 5 % w/v) coarse secondary particles which start to agglomerate can be observed (see Figure 2(b-d)). When the concentration increases (to 10 – 20 % w/v) the needles are more defined and form round sponge-shaped aggregates, as are visible in Figure 2(e-g). These differences in particle habit compared to the non-templated control are in agreement with change in relative peak intensities observed by XRD (see Figure 1a, where the relative reflection intensities at 11.66 and 20.76 ° 2θ vary).

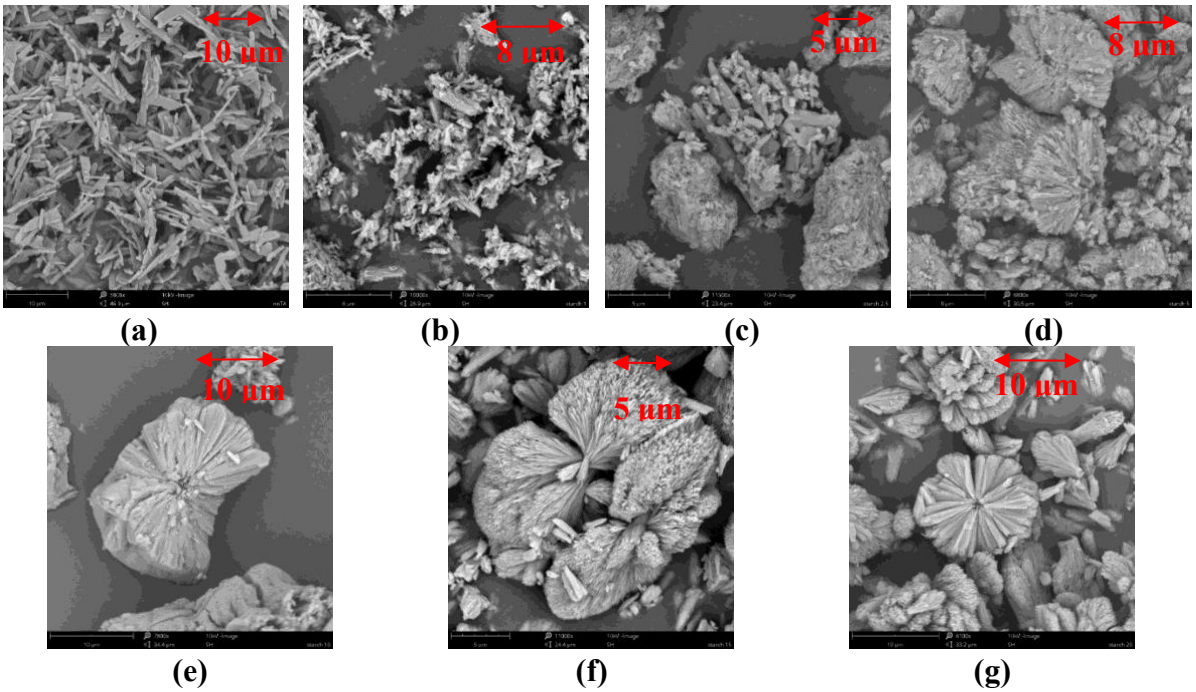

Figure 2. SEM images of gypsum seeds synthesised with different amounts of starch: (a) 0% (w/v); (b) 1% (w/v); (c) 2.5% (w/v); (d) 5% (w/v); (e) 10% (w/v); (f) 15% (w/v); and (g) 20% (w/v)

Setting times were quantified using the knife method (see Section 2.3.3). The results are depicted in Figure 3 and detailed in Table S 6.

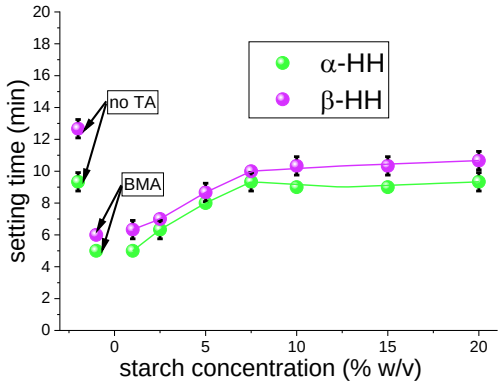

Figure 3. Setting times for α- and β-hemihydrate with seeds produced with starch

Where no accelerator is used, the setting time is 9 ± 1 min and 13 ± 1 min for α-HH and β-HH respectively. The commercial BMA accelerant (see Figure S 3(a)) gives setting times of 5 ± 0 and 6 ± 0 min. An increase in the concentration of starch used for preparing seeds raised the setting time for both hemihydrates, which increases from 5 ± 0 min and 6 ± 1 min (α- and β-HH respectively) at 1% w/v to 9 ± 1 min and 11 ± 1 min when the starch concentration is 20% w/v. This can be attributed to the increasing level of aggregation observed as the starch concentration used for templating rises.

Unfortunately, there is no literature with which to compare the setting times of HH obtained when different shape/sizes of gypsum seeds are used. However, templating is clearly a very powerful technique which allows a change of particle morphology. The shortest setting times are observed for low starch concentrations, where there are only rod-shaped particles present and minimal aggregation. These materials perform as well as the commercial BMA. The latter comprises a range of particle sizes and shapes (Figure S 3(a)), and is highly inhomogeneous. It appears that a bottom-up template synthesis of needle-shaped particles could deliver the same performance without the concerns of batch-to-batch variability that currently cause major issues in gypsum factories worldwide. A grinding process will produce a number of efficient seeds, comprising small particles having the right size and shape to become crystallization seeds. This number depends on many operational parameters: for instance, the nature of the raw gypsum source (e.g. density of the rock, type of crystallization, particle size distribution

before grinding), the milling equipment used, and the grinding energy. Thus, the weight percentage of active seeds in any batch (and hence the efficacy of the BMA) varies significantly not only from factory to factory but also from day to day at a given production site.

3.2. Liquid seeds from dry seeds

The seeds prepared with starch as templating agent were highly aggregated at higher concentrations (Figure 2). It was expected that suspending them in SSS and sonicating should result in the breakdown of these aggregates and allow the isolation of individual particles of gypsum. This should in turn increase the number of seeds available to accelerate the HH hydration process. The effect of the suspension and sonication process was thus explored. TEM images of samples prepared by sonicating the dry material in SSS for 10 min are presented in Figure 4. At the lower starch concentrations, the aggregates have clearly been broken up after sonication (Figure 4(a-c)). However, the formulations prepared with increased starch concentrations (above 10 % w/w) remain aggregated even after sonication (Figure 4(d-f). The suspension and sonication process was also applied to the commercially used BMA seeds. SEM and TEM images are presented in Figure S 3, and again reveal that effective separation of the primary particles can be achieved.

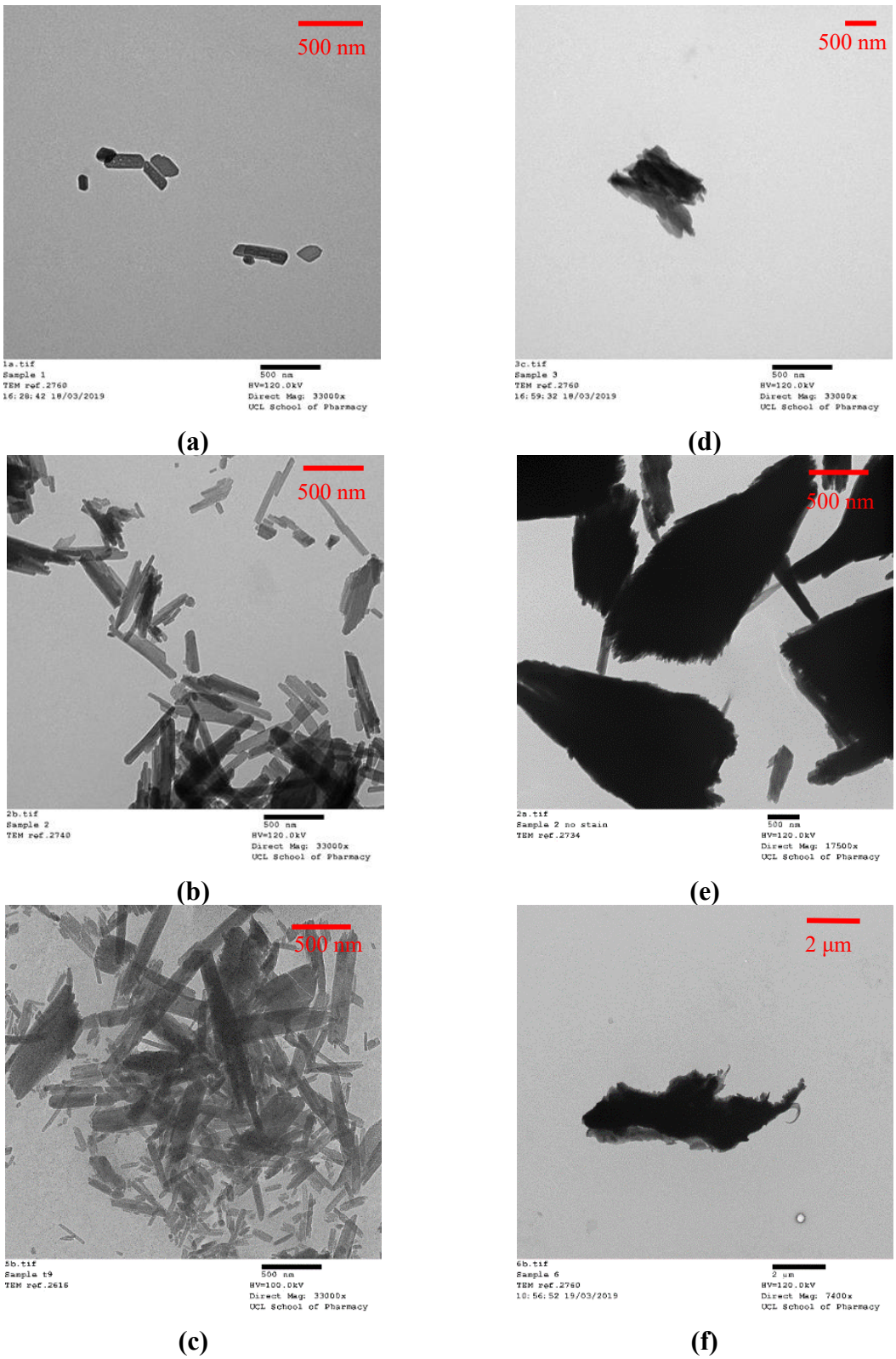

Figure 4. TEM images of gypsum seeds synthesized with different concentrations of starch (a) 1 % (w/v); (b) 2.5 % (w/v); (c) 5 % (w/v); (d) 10 % (w/v); (e) 15 % (w/v); and (f) 20 % (w/v) after sonication in SSS.

Setting time results for the liquid seeds are depicted graphically in Figure 5 and detailed in Table S 7. After sonication and suspension, the setting times are much more rapid than those obtained with the analogous dry seed formulations, and indeed better than with the commercial BMA. The seeds prepared with 5 % w/v starch show the best performance overall here. The LS are hence potent in accelerating the conversion from HH to gypsum, and offer considerable benefits over the dried particles. Unfortunately, the two-step synthesis is complex, time consuming and not cost efficient. Therefore, there is a need to design a one-step process which could speed up and lower the cost of the production of LS.

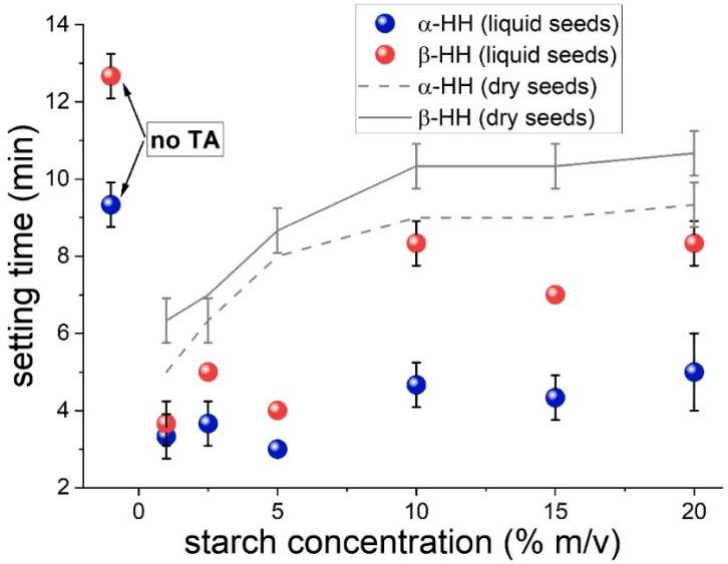

Figure 5. Setting times for α- and β-HH with liquid seeds produced with starch as templating agent

3.3.One step synthesis of liquid seeds

Here we sought to develop a rapid, one-step, synthesis for liquid seeds, such that they could be directly added to a production line. This is complicated by the requirement to use ethanol in the synthesis process, since the presence of ethanol at > 1% v/v will halt or delay the HH hydration process. To overcome this issue, elevated temperature syntheses were explored. First, a GC method was developed to quantify the ethanol concentration in the reaction matrix (see Figure S 4 and Figure S 5). Using this, it was determined that after 4 h at 80 °C or 6 h at

75 ºC no residual ethanol could be detected (Figure S 6). The generation of seeds using these protocols was thus explored, in addition to a synthesis where the seeds were precipitated at room temperature and then heated at 80 ºC for 4 h. Starch was added at a concentration of 5% w/v to template the seeds.

After the synthesis was finished the volume of the solvent remaining was checked and the weight of the dry seeds quantified after washing and air drying. The yields in Table 2 were obtained. It is clear that the use of elevated temperatures reduces the yield, as is to be expected since the solubility of gypsum in water will increase with temperature.

Table 2. Dry seed yields from one-step synthesis in the presence of 5 % w/v starch

Sample	**Yield [%]**
RT	93 ± 4
RT-80 ºC	56 ± 1
75 ºC	42 ± 5
80 ºC	38 ± 3

SEM images show that the gypsum seeds prepared at room temperature with 5 % w/v starch comprise needle particles which are agglomerated into a sponge shaped aggregate (Figure 2(d)). When the seeds are synthesized at RT and then the temperature is raised to 80 ºC the dried product resembles that synthesized at RT (Figure 6(a)). Considering the elevated temperature reactions, the product generated at 75 ºC (Figure 6(b)) shows flat rhomboid particles and some aggregates are visible in the form of flower-shapes. At 80 ºC (Figure 6(c)) this phenomenon is not visible and only flat rhomboid particles are seen. It is worth noticing that these particles are very different to those synthesized at room temperature, and there is a distinct change in shape from agglomerated needles (Figure 2(d)) to rhomboid shape particles (Figure 6(b,c)). Also, it seems that the particles synthesized at high temperature are much larger

than those synthesized at RT. This is expected since the growth kinetics of forming gypsum seeds increase with temperature and as result bigger crystals are formed.[24] These findings are perhaps indicative that the samples prepared at high temperatures may be ineffective as seeds, while those from the RT-80 °C reaction should behave similarly to those produced at RT.

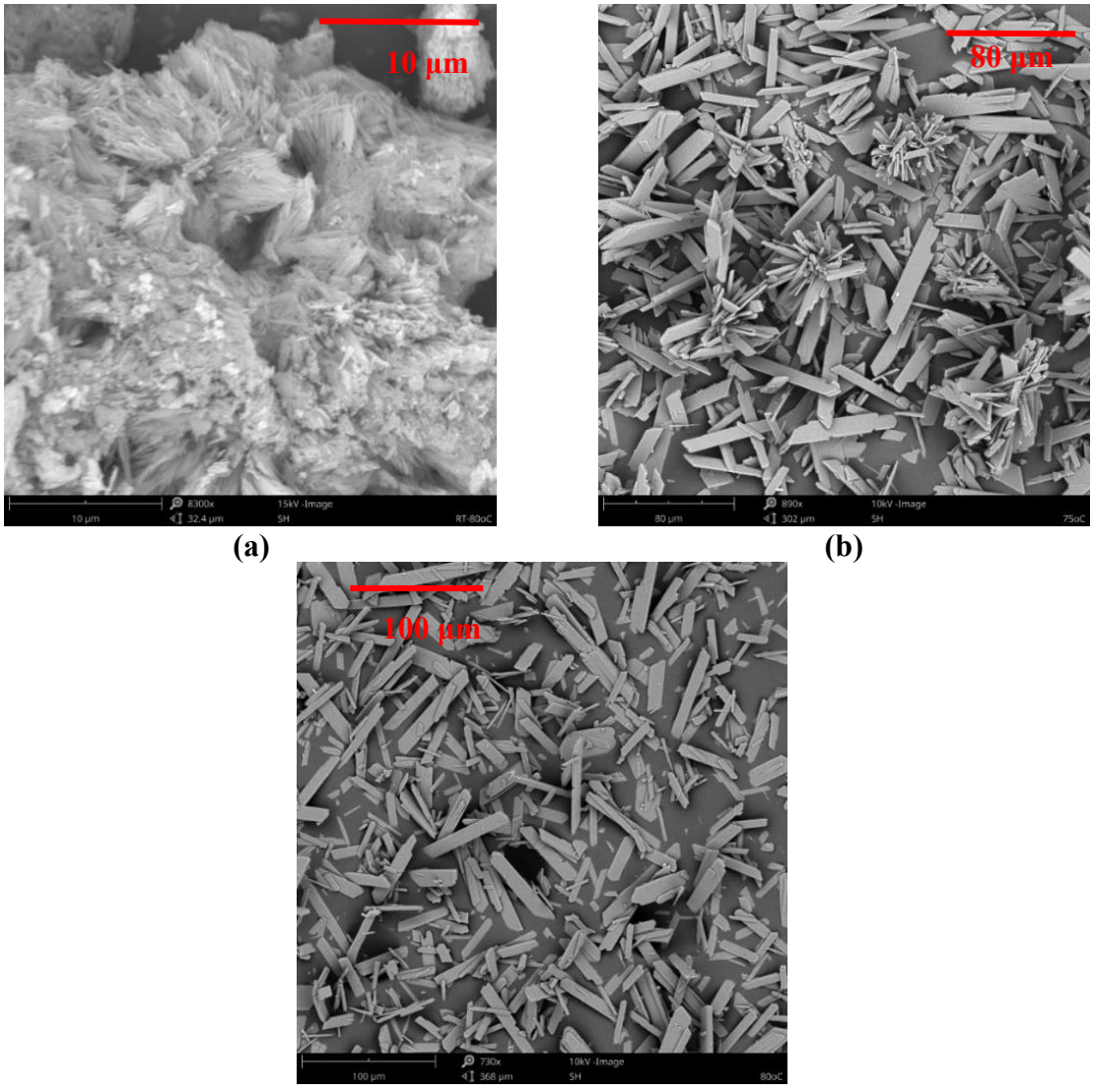

(a) **(b)**

(c)

Figure 6. SEM images of gypsum seeds synthesized with 5 % w/v starch at (a) RT-80 ºC; (b) 75 ºC; and (c) 80 ºC

Given the use of elevated temperatures in the one-step seeds synthesis, it was necessary to investigate the nature of the product formed. XRD patterns (Figure 7(a)), IR spectra (Figure

7(b), and TGA data (Figure 7(c)) confirm that in all three cases gypsum particles were synthesized. The relative intensities of the reflections in XRD can be seen to be different at the various temperatures, consistent with the different particle habits observed in Figure 6. It should be noted that the anhydrite has lower solubility than CSD above ca. 55 °C and thus might be expected to form from solution. However, owing to kinetic and thermodynamic inhibition, the literature reports that gypsum forms predominantly until the temperature of the system reaches 99 °C.[25]

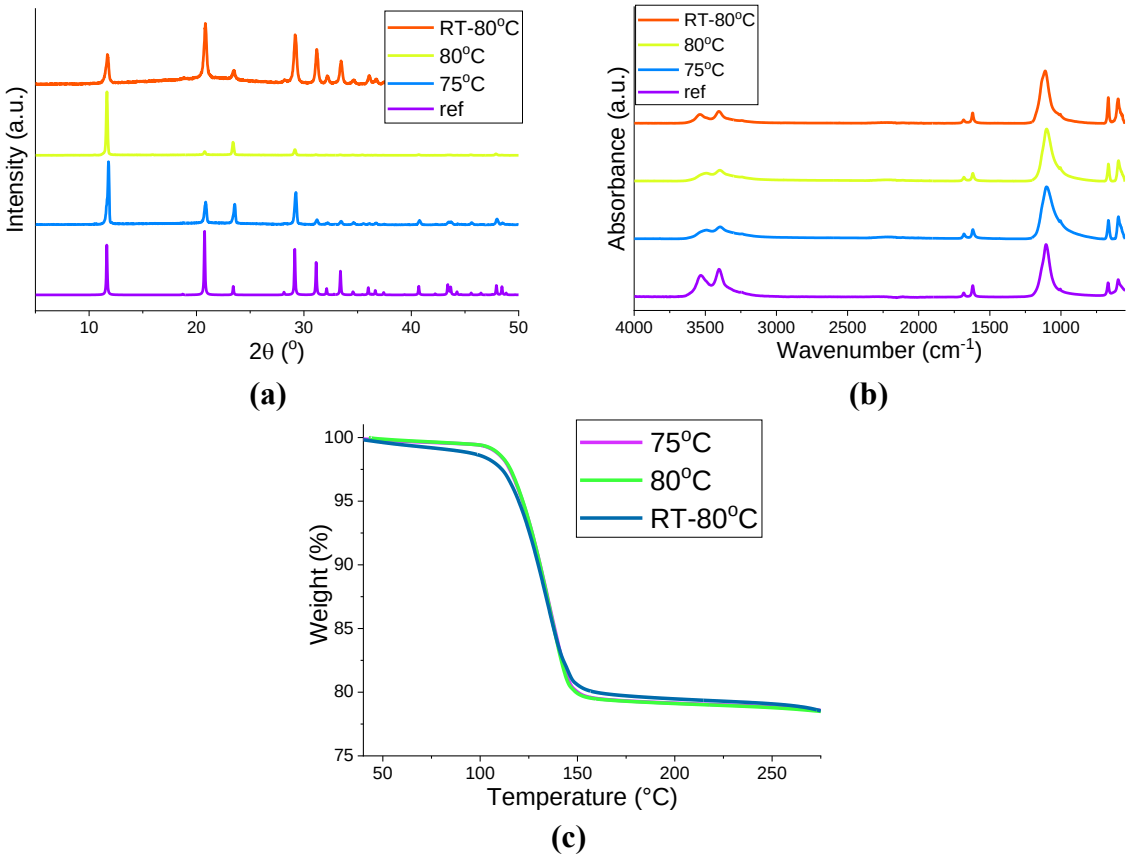

Figure 7. Data patterns for gypsum seeds synthesized at 75 °C, 80 °C and RT-80 °C. (a) XRD patterns; (b) IR spectra; (c) TGA thermograms. The mass losses in the latter are 21.12 ± 0.01, 21.21 ± 0.02 and 20.98 ± 0.03 % for the samples synthesised at 75 °C, 80 °C and RT-80 °C respectively.

The setting time data for the one-step seeds are depicted in Figure 8, with the full results listed in Table S 8.

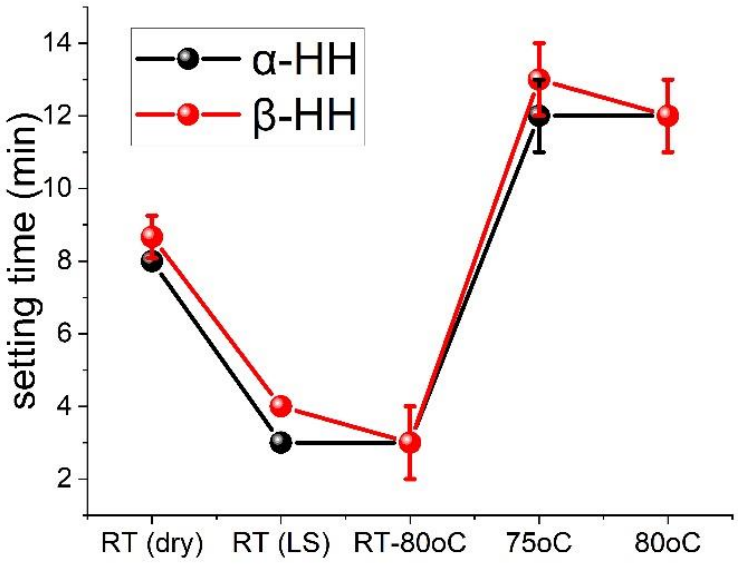

Figure 8. Setting time for liquid seeds prepared in a single-reaction step with elevated temperatures.

The setting times for the seeds synthesized at 75 °C and 80 °C are very long. This is likely to be a result of the large rhomboid particles which are generated at these temperatures. In contrast, if the seeds are synthesized at RT and the temperature is then increased to 80 °C (and held for a period of four hours to allow the ethanol to evaporate) the generated LS give a short setting time for both α- and β-HH. The setting time for the liquid seeds synthesized at RT – 80 °C is the same as that for those prepared at RT. This is expected as both syntheses (RT and RT – 80 °C) produce seeds which are very similar in size and shape after drying. Thus, when removing ethanol from the system it is clear that this process should be carried out after the synthesis is completed to achieve seeds with accelerating properties. The optimal route developed here offers a simple route for LS to be synthesised in a single step, and then added to an industrial production line. The ethanol used in synthesis could be recovered and recycled for use in subsequent reactions.

3.4.Mechanical strength

The use of starch templated LS is able to dramatically accelerate the HH to CSD setting process, and suspension seeds can be generated in a single step. This is potentially very useful in industrial processes. However, the effect of the seeding on the mechanical properties of the CSD product must also be considered. The mechanical properties of beams formed with BMA acceleration were first determined as reference values. The data are shown in Figure S 7. The bending test results are very different for the two types of HH (Figure S 7(a,b)). It seems that in the α-HH case an increase in BMA content causes the beams to break at a lower force, whereas the opposite trend is seen with the β-HH. With an increasing amount of BMA we have an increasing number of nucleation sites. Hence, more crystals start to form and crystal growth rather than nucleation is likely to be the rate determining step in the hydration reaction, and the product will comprise a larger number of smaller crystals. CSD from α-HH is known to have more densely intertwined crystals, which are responsible for its strength.[26,27] The difference in strength between the two forms of CSD is also in part a result of the different ratios of water to the HH used in beam fabrication.

In Figure S 7(c,d) it can be seen that with an increased amount of BMA the compression strength rises for both α- and β-HH. This is because there are a larger number of smaller crystals in the beams with higher concentrations of BMA. As the crystals are much more closely packed, this gives the beams more strength under compression. The α-HH beams are much stronger (38-44 MPa), while a force of only 8-13 MPa is need to break the β-HH beams.

Mechanical strength test results for the beams synthesized with LS are shown in Figure 9 (with further data in Table S 9 and Table S 10). The beams were prepared with LS at a seed concentration of 0.2 % w/w with respect to the mass of α- and β-HH. The data for beams prepared with dry BMA at the same concentration are included for comparison purposes.

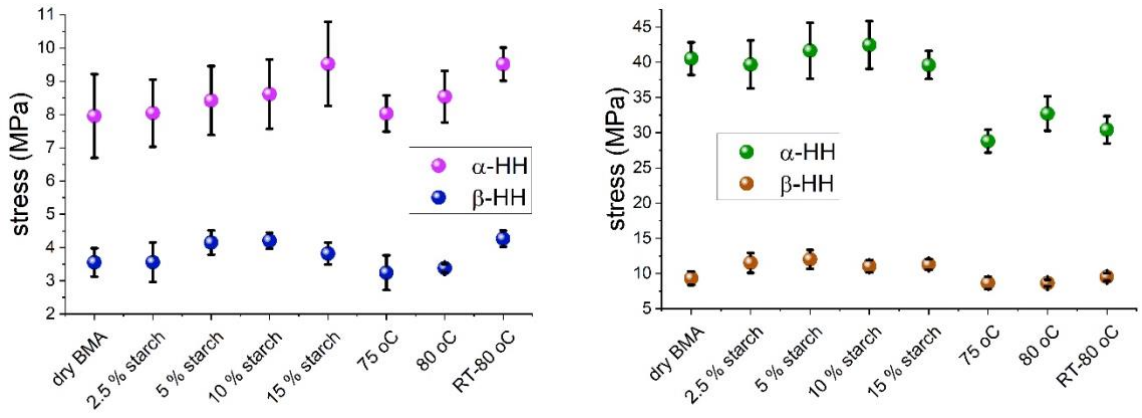

Figure 9. Bending stress (a) and compression (b) tests for beams formed from α-HH and β-HH with the starch-templated liquid seeds.

When LS are used, the beams have the same (or slightly higher) mechanical strength (both under bending and compression) as those made with the equivalent amount of BMA (Figure 9). This is important, as it indicates that use of LS does not change the mechanical properties of the beams and hence LS could be used in the production line as an alternative to BMA. The seeds prepared in the RT-80 ºC process also result in beams with very similar mechanical properties to those made with BMA, except in the compression test on α-HH beams. Here, the mechanical strength is somewhat reduced. The reasons for this are not clear, and required further exploration. However, overall the findings are very promising for using the RT-80 °C route to generate LS in a single step, because most global plasterboard production focuses on the β-HH.

4. Conclusions

This study explores the bottom-up precipitation of gypsum particles, using starch as a templating agent. We show that the use of the templating agent provides good control over particle morphology, but upon drying the particles tend to aggregate. This reduces their ability to accelerate the industrially important hydration reaction of $CaSO_4 \cdot 0.5H_2O$ to $CaSO_4 \cdot 2H_2O$.

Resuspending the particles with sonication results in the aggregates being broken up and leads to a marked reduction in the hydration time. However, such a two-stage process to seed production is unlikely to be feasible for industrial translation owing to its complexity. The gypsum precipitation process requires the use of ethanol in the synthesis, which means that the reaction product cannot be directly added to an industrial production line as the ethanol would cause the hydration reaction to slow significantly or halt. To overcome these challenges, we developed a simple one-step process where seeds were precipitated and then the suspension heated to remove the ethanol. This results in highly potent seeds, which perform better than a commercial gypsum accelerant in speeding up the hemihydrate to dihydrate hydration reaction.

5. Acknowledgements

We thank Etex Group for award of a PhD studentship to Sebastian J Gurgul, and Miss Satinder Sembi and Dr Rui Manuel Jesus Lopes for assistance with GC measurements.

6. Abbreviations

BMA	Ball-milled accelerant
CSD	Calcium sulfate dihydrate
GC	Gas chromatography
HH	Calcium sulfate hemihydrate
IR	Infrared
LS	Liquid seeds
PAA	Polyacrylic acid
RT	Room temperature
SEM	Scanning Electron Microscopy
S.D.	Standard deviation
TA	Templating agent
TEM	Transmission electron microscopy
TGA	Thermogravimetric analysis
XRD	X-ray diffraction

7. References

(1) John, G.; Lidgard, P. Carbon Plaster Board - Patent WO2011078708 A1, 2010.

(2) Laurent, C. Investigating the Fire Resistance of Ultra Lightweight Foam Concrete. *Rev. Tec. la Fac. Ing. Univ. del Zulia* **2014**, *37* (1), 11–18.

(3) Thomas, G. Thermal Properties of Gypsum Plasterboard at High Temperatures. *Fire Mater.* **2002**, *26* (1), 37–45. https://doi.org/10.1002/fam.786.

(4) Yu, Q. L.; Brouwers, H. J. H. Microstructure and Mechanical Properties of β-Hemihydrate Produced Gypsum: An Insight from Its Hydration Process. *Constr. Build. Mater.* **2011**, *25* (7), 3149–3157. https://doi.org/10.1016/j.conbuildmat.2010.12.005.

(5) Wirsching, F. *Calcium Sulfate*; Wiley: Weinheim, Germany, 2002; Vol. 92. https://doi.org/10.1002/3527600418.

(6) Amathieu, L.; Boistelle, R. Improvement of the Mechanical Properties of Set Plasters by Means of Four Organic Additives Inducing {101} Faces. *J. Cryst. Growth* **1986**, *79* (1–3), 169–177. https://doi.org/10.1016/0022-0248(86)90432-X.

(7) Otto L. Dozsa. Accelerator for Gypsum Plaster and Process of Manufacture - US4681644, 1987.

(8) Campbell, F. H.; Piasecki, R. J.; Kingston, L. W.; Burkard, E. A. Gypsum Set Accelerator and Method of Making the Same Patent: US 6221151 B1, 2001.

(9) Immordino, S. C.; Espinoza, T.; Stevens, R. B.; Miller, C. J. Efficient Set Accelerator for Plaster Patent: US 6379458, 2002.

(10) Campbell, Frank, H.; Pasecki, Robert, J.; Kingston, Larry, W.; Burkard, Edward, A. Method of Making a Gypsum Set Acceletator - Patent EP 1 204 614 B1. EP 1 204 614 B1, 2004.

(11) Titiz-Sargut, S.; Sayan, P.; Avcı, B. Influence of Citric Acid on Calcium Sulfate Dihydrate Crystallization in Aqueous Media. *Cryst. Res. Technol.* **2007**, *42* (2), 119–126. https://doi.org/10.1002/crat.200610783.

(12) Sargut, S. T.; Sayan, P.; Kiran, B. Gypsum Crystallization in the Presence of Cr3+ and Citric Acid. *Chem. Eng. Technol.* **2010**, *33* (5), 804–811. https://doi.org/10.1002/ceat.200900567.

(13) Trivedi, T. J.; Pandya, P.; Kumar, A. Effect of Organic Additives on the Solubility Behavior and Morphology of Calcium Sulfate Dihydrate (Gypsum) in the Aqueous Sodium Chloride System and Physicochemical Solution Properties at 35 °C. *J. Chem. Eng. Data* **2013**, *58* (3), 773–779. https://doi.org/10.1021/je3012887.

(14) Badens, E.; Veesler, S.; Boistelle, R. Crystallization of Gypsum from Hemihydrate in Presence of Additives. *J. Cryst. Growth* **1999**, *198–199*, 704–709. https://doi.org/10.1016/S0022-0248(98)01206-8.

(15) Lioliou, M. G.; Paraskeva, C. A.; Koutsoukos, P. G.; Payatakes, A. C. Calcium Sulfate Precipitation in the Presence of Water-Soluble Polymers. *J. Colloid Interface Sci.* **2006**, *303* (1), 164–170. https://doi.org/10.1016/j.jcis.2006.07.054.

(16) Chairam, S.; Poolperm, C.; Somsook, E. Starch Vermicelli Template-Assisted Synthesis of Size/Shape-Controlled Nanoparticles. *Carbohydr. Polym.* **2009**, *75* (4), 694–704. https://doi.org/10.1016/j.carbpol.2008.09.022.

(17) Rosseto, M.; V.T. Rigueto, C.; D.C. Krein, D.; P. Balbé, N.; A. Massuda, L.; Dettmer, A. Biodegradable Polymers: Opportunities and Challenges. In *Organic Polymers*; IntechOpen, 2019. https://doi.org/10.5772/intechopen.88146.

(18) Jiang, T.; Duan, Q.; Zhu, J.; Liu, H.; Yu, L. Starch-Based Biodegradable Materials: Challenges and Opportunities. *Adv. Ind. Eng. Polym. Res.* **2020**, *3* (1), 8–18. https://doi.org/10.1016/j.aiepr.2019.11.003.

(19) Vroman, I.; Tighzert, L. Biodegradable Polymers. *Materials (Basel).* **2009**, *2* (2), 307–344. https://doi.org/10.3390/ma2020307.

(20) Fernández-Martínez, A.; Cuello, G. J.; Johnson, M. R.; Bardelli, F.; Román-Ross, G.; Charlet, L.; Turrillas, X. Arsenate Incorporation in Gypsum Probed by Neutron, X-Ray Scattering and Density Functional Theory Modeling. *J. Phys. Chem. A* **2008**, *112* (23), 5159–5166. https://doi.org/10.1021/jp076067r.

(21) Wang, Y.-W.; Meldrum, F. C. Additives Stabilize Calcium Sulfate Hemihydrate (Bassanite) in Solution. *J. Mater. Chem.* **2012**, *22* (41), 22055. https://doi.org/10.1039/c2jm34087a.

(22) Al-Jobouri, H. A. FTIR Spectroscopy for Gypsum after Treatment with Steam Pressure. *J. Al-Nahrain Univ. Sci.* **2011**, *14* (2), 123–130. https://doi.org/10.22401/jnus.14.2.16.

(23) Liu, Y. Raman, Mid-IR, and NIR Spectroscopic Study of Calcium Sulfates and Mapping Gypsum Abundances in Columbus Crater, Mars. *Planet. Space Sci.* **2018**, *163*, 35–41. https://doi.org/10.1016/j.pss.2018.04.010.

(24) Van Driessche, A. E. S.; García-Ruiz, J. M.; Delgado-López, J. M.; Sazaki, G. In Situ Observation of Step Dynamics on Gypsum Crystals. *Cryst. Growth Des.* **2010**, *10* (9), 3909–3916. https://doi.org/10.1021/cg100323e.

(25) Ossorio, M.; Van Driessche, A. E. S.; Pérez, P.; García-Ruiz, J. M. The Gypsum-Anhydrite Paradox Revisited. *Chem. Geol.* **2014**, *386*, 16–21. https://doi.org/10.1016/j.chemgeo.2014.07.026.

(26) Follner, S.; Wolter, A.; Preusser, A.; Indris, S.; Silber, C.; Follner, H. The Setting Behaviour of α- and β-CaSO4 · 0,5 H2O as a Function of Crystal Structure and Morphology. *Cryst. Res. Technol.* **2002**, *37* (10), 1075–1087. https://doi.org/10.1002/1521-4079(200210)37:10<1075::AID-CRAT1075>3.0.CO;2-X.

(27) Singh, N. B. B.; Middendorf, B. Calcium Sulphate Hemihydrate Hydration Leading to Gypsum Crystallization. *Prog. Cryst. Growth Charact. Mater.* **2007**, *53* (1), 57–77. https://doi.org/10.1016/j.pcrysgrow.2007.01.002.

Table of contents graphic